

# Slater-Pauling Behavior and Origin of the Half-Metallicity of the Full-Heusler Alloys

I. Galanakis\* and P. H. Dederichs

*Institut für Festkörperforschung, Forschungszentrum Jülich, D-52425 Jülich, Germany*

N. Papanikolaou

*Fachbereich Physik, Martin-Luther Universität, Halle-Wittenberg, D-06099 Halle, Germany  
Institute of Materials Science, NCSR “Demokritos,” 153 10 Aghia Paraskevi, Athens, Greece*

(Dated: January 28, 2022)

Using the full-potential screened Korringa-Kohn-Rostoker method we study the full-Heusler alloys based on Co, Fe, Rh and Ru. We show that many of these compounds show a half-metallic behavior, however in contrast to the half-Heusler alloys the energy gap in the minority band is extremely small due to states localized only at the Co (Fe, Rh or Ru) sites which are not present in the half-Heusler compounds. The full-Heusler alloys show a Slater-Pauling behavior and the total spin-magnetic moment per unit cell ( $M_t$ ) scales with the total number of valence electrons ( $Z_t$ ) following the rule:  $M_t = Z_t - 24$ . We explain why the spin-down band contains exactly 12 electrons using arguments based on the group theory and show that this rule holds also for compounds with less than 24 valence electrons. Finally we discuss the deviations from this rule and the differences compared to the half-Heusler alloys.

PACS numbers: 71.20.Be, 71.20.Lp

## I. INTRODUCTION

The increased interest in the field of magnetoelectronics or spinelectronics during the last decade<sup>1</sup> intensified the research on the so-called half-ferromagnetic materials. The latter ones present a gap in the minority band and thus can be used as perfect spin-filters or to enhance the performance of spin-dependent devices as electrons at the Fermi level are 100% spin polarized. The first material which has been predicted to be a half-ferromagnet was the half-Heusler alloy NiMnSb found by de Groot and collaborators<sup>2</sup> in 1983. This prediction has been verified also by other authors<sup>3,4,5</sup> and the half-ferromagnetic character has been also well established experimentally both by using positron annihilation experiments<sup>6</sup> or inverse photoemission.<sup>7</sup> Recently there is an increased interest on thin films of this material both experimentally<sup>8</sup> and using first-principle calculations.<sup>9,10</sup>

Although the half-Heusler alloys like NiMnSb have attracted a lot of interest, the second family of Heusler compounds, the so-called full-Heusler alloys have been studied much more extensively due to the existence of diverse magnetic phenomena,<sup>11,12</sup> mainly the transition from a ferromagnetic phase to an antiferromagnetic one by changing the concentration of the carriers.<sup>13</sup> The full-Heusler alloys have the type  $X_2YZ$  (see Fig.1) and they crystallize in the  $L2_1$  structure which consists of four fcc sublattices. Webster and Ziebeck<sup>14</sup> were the first to synthesize full-Heusler alloys containing Co, and Ishida and collaborators<sup>15,16</sup> have proposed that the compounds of the type  $Co_2MnZ$ , where Z stands for Si and Ge, are also half-ferromagnets. Also the Heusler alloys of the type  $Fe_2MnZ$  have been proposed to show half-ferromagnetism.<sup>17</sup> But Brown *et al.*<sup>18</sup> using polarized neutron diffraction measurements have shown that there is a finite very small spin-down density of states

(DOS) at the Fermi level instead of an absolute gap in agreement with the *ab-initio* calculations of Kübler *et al.* for the  $Co_2MnAl$  and  $Co_2MnSn$  compounds.<sup>13</sup> Recently, Ambrose *et al.*<sup>19</sup> managed to grow a  $Co_2MnGe$  thin film on a GaAs(001) substrate by molecular beam epitaxy and have proven the creation of domains during the growth.<sup>20</sup> Raphael *et al.* have grown both thin films and single crystals of  $Co_2MnSi$ .<sup>21</sup> Although these films were found to adopt the  $L1_1$  structure there was a strong disorder between the Mn and Co sites even in the case of bulk  $Co_2MnSi$ .<sup>22</sup> Also, Geiersbach and collaborators have grown (110) thin films of  $Co_2MnSi$ ,  $Co_2MnGe$  and  $Co_2MnSn$  using a metallic seed on top of a MgO(001) substrate,<sup>23</sup> Finally there also exist first-principles calculations for the (001) surface of such an alloy.<sup>10,24</sup>

Suits<sup>25</sup> was the first to synthesize compounds of the form  $Rh_2MnZ$ , where Z stands for Al, Ga, In, Tl, Ge, Sn and Pb. They all crystallize in the  $L2_1$  structure but the compounds containing a II type *sp* element show considerable disorder between the *sp* atom and the Mn site. They are all ferromagnets and the compounds containing Ge, Sn and Pb have a Curie temperature above room temperature. Kanomata *et al.*<sup>26</sup> have grown crystals of the type  $Ru_2MnZ$ , where Z stands for Si, Ge, Sn and Sb. Gotoh *et al.*<sup>27</sup> have shown that these alloys are antiferromagnets with Néel temperatures near room temperature, and Ishida *et al.*<sup>28</sup> using first-principles calculations demonstrated that the ground state is antiferromagnetic with the Mn atoms in the (111) plane being antiferromagnetically coupled to the neighboring (111) planes.

In this contribution we study the full-Heusler alloys based on Co, Fe, Ru and Rh by extending our work on the half-Heusler alloys (see Ref. 5) and on the transition metal monoarsenides (see Ref. 29). To perform the calculations we have used the full-potential screened Korringa-Kohn-Rostoker (FSKKR) Green's function method<sup>30</sup> in

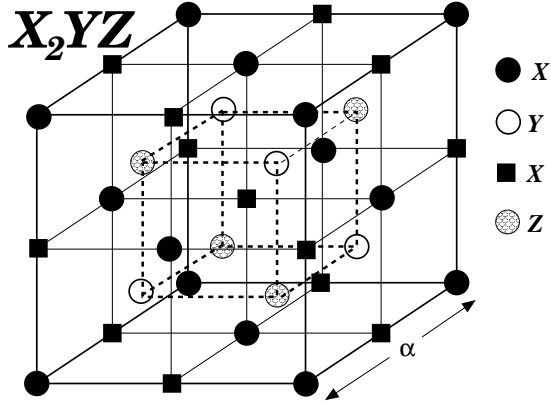


FIG. 1: Schematic representation of the  $L2_1$  structure. The lattice consists of 4 fcc sublattices. The unit cell is that of a fcc lattice with four atoms as basis: X at  $(0\ 0\ 0)$  and  $(\frac{1}{2}\ \frac{1}{2}\ \frac{1}{2})$ , Y at  $(\frac{1}{4}\ \frac{1}{4}\ \frac{1}{4})$  and Z at  $(\frac{3}{4}\ \frac{3}{4}\ \frac{3}{4})$  in Wyckoff coordinates.

TABLE I: Calculated spin magnetic moments in  $\mu_B$  using the experimental lattice constants (see Ref. 11) for the  $\text{Co}_2\text{MnZ}$  compounds, where Z stands for the *sp* atom.

$m^{spin}(\mu_B)$	Co	Mn	Z	Total
$\text{Co}_2\text{MnAl}$	0.768	2.530	-0.096	3.970
$\text{Co}_2\text{MnGa}$	0.688	2.775	-0.093	4.058
$\text{Co}_2\text{MnSi}$	1.021	2.971	-0.074	4.940
$\text{Co}_2\text{MnGe}$	0.981	3.040	-0.061	4.941
$\text{Co}_2\text{MnSn}$	0.929	3.203	-0.078	4.984

conjunction with the local spin density approximation.<sup>31</sup> The details of our calculations have been already described in Ref. 5. For all the compounds under study we have used the experimental lattice constants,<sup>11,26</sup> and have assumed that they are all ferromagnets. In Section II we present the properties of the  $\text{Co}_2\text{MnZ}$  compounds. In Section III we discuss the origin of the gap in these compounds and the Slater-Pauling (SP) behavior of the total moments. In Section IV we present our results for some other interesting systems. Finally in Section V we summarize our results and conclude.

## II. $\text{Co}_2\text{MnZ}$ COMPOUNDS

The first family of alloys, we will be interested in, are the compounds containing Co and Mn as they are the ones that have attracted most of the attention. They are all strong ferromagnets with high Curie temperatures (above 600 K) and except the  $\text{Co}_2\text{MnAl}$  they show very little disorder.<sup>11</sup> They adopt the  $L2_1$  structure, which we present in Fig. 1. Each Mn or *sp* atom has eight Co atoms as first neighbors sitting in an octahedral symmetry position, while each Co has four Mn and four *sp* atoms as first neighbors and thus the symmetry of the crystal is reduced to the tetrahedral one. The Co atoms occupying the two different sublattices are chemically equivalent as

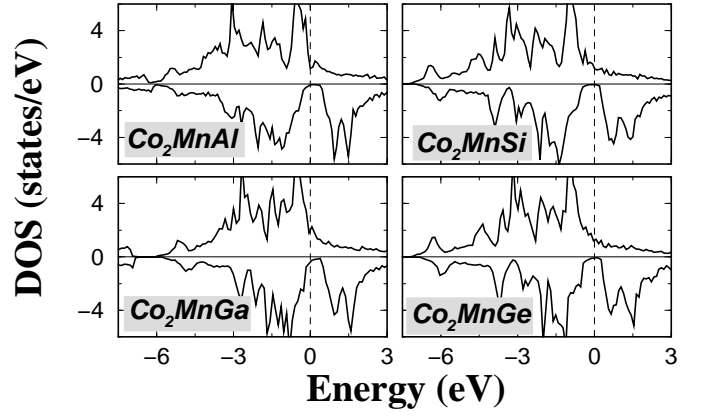


FIG. 2: Calculated spin-projected DOS for the  $\text{Co}_2\text{MnZ}$  compounds, where Z stands for Al, Ga, Si and Ge. They all possess a finite very small spin-down DOS around the Fermi level.

the environment of the one sublattice is the same as the environment of the second one but rotated by  $90^\circ$ . The occupancy of two fcc sublattices by Co (or in general by X) atoms distinguishes the full-Heusler alloys with the  $L2_1$  structure from the half-Heusler compounds with the  $C1_b$  structure, like *e.g.*  $\text{CoMnSb}$ , where only one sublattice is occupied by Co atoms and the other one is empty. Although in the  $L2_1$  structure, the Co atoms are sitting on second neighbor positions, their interaction is important to explain the magnetic properties of these compounds as we will show in the next section. In Fig. 2 we have gathered the spin-resolved total density of states (DOS) for the  $\text{Co}_2\text{MnAl}$ ,  $\text{Co}_2\text{MnGa}$ ,  $\text{Co}_2\text{MnSi}$  and  $\text{Co}_2\text{MnGe}$  compounds calculated using the FSKKR and in Table I the atom-projected and the total spin magnetic moment for these four compounds and for  $\text{Co}_2\text{MnSn}$ . Firstly as shown by photoemission experiments by Brown *et al.*<sup>32</sup> in the case of  $\text{Co}_2\text{MnSn}$  and verified by our calculations the valence band extends 5 eV below the Fermi level and the spin-up DOS shows a large peak just below the Fermi level for these compounds. Although Ishida *et al.*<sup>15</sup> have predicted them to be half-ferromagnets with small spin-down gaps ranging from 0.1 to 0.3 eV depending on the material, within our calculations we find that the Fermi level falls within a region of very small spin-down DOS for all these compounds. Our results agree with the calculations of Kübler *et al.*<sup>13</sup> who studied the  $\text{Co}_2\text{MnAl}$  and  $\text{Co}_2\text{MnSn}$  compounds using the Augmented Spherical Wave (ASW) method and found also a very small spin-down DOS at the Fermi level and not a real gap. The reason of this pseudogap can be found in Fig. 3 where we have drawn the band structure for the minority electrons in the case of the  $\text{Co}_2\text{MnGe}$  compound (our spin-down band structure is similar to the one obtained for  $\text{Co}_2\text{FeGa}$  and  $\text{Mn}_2\text{VAl}$  in Refs. 33 and 34 respectively). We see that the Fermi level touches the highest occupied bands at the  $\Gamma$  point and the lowest unoccupied bands at the X point and thus the indirect gap found in the

half-Heusler alloys<sup>2</sup> is practically destroyed in these materials but there is still a reasonably large direct gap at the W, K and X points. However we should mention that if we considerably enlarge the figure with the band structure, it can be seen that the bands do not really touch the Fermi level but there is a very small indirect gap of the order of 0.001 eV and thus the minimum of the minority unoccupied bands at X and the maximum of the occupied bands at the  $\Gamma$  point are not degenerated. Our calculations include relativistic effects only within the scalar-relativistic approximation, thus effects like the spin-orbit coupling can lift the bands degeneracy and might even destroy the indirect gap. However we should mention that in case of sufficient large band gaps like in the case of NiMnSb, the spin-orbit coupling does not destroy the half-metallicity.<sup>5</sup>

In the case of the half-Heusler alloys<sup>5</sup> like NiMnSb the Mn spin magnetic moment is very localized due to the exclusion of the spin-down electrons at the Mn site and amounts to about  $3.7 \mu_B$  in the case of NiMnSb. In the case of CoMnSb the increased hybridization between the Co and Mn spin-down electrons decreased the Mn spin moment to about  $3.2 \mu_B$ . In the case of the full-Heusler alloys each Mn atom has eight Co atoms as first neighbors instead of four as in CoMnSb and the above hybridization is very important decreasing even further the Mn spin moment to less than  $3 \mu_B$  except in the case of Co<sub>2</sub>MnSn where it is comparable to the CoMnSb compound. The Co atoms are ferromagnetically coupled to the Mn spin moments and they possess a spin moment that varies from  $\sim 0.7$  to  $1.0 \mu_B$ , while the *sp* atom has a very small negative moment which is one order of magnitude smaller than the Co moment. The negative sign of the induced *sp* moment characterizes most of the studied full and half Heusler alloys with very few exceptions.

Another important point is that in half-metallic materials like the ones studied here the total spin moment should be an integer number since both the total number of valence electrons as well as the number of occupied minority states are integers. However our results in Table I do not give integer numbers for the total moments, but slight deviations of about  $0.05 \mu_B$ . This does not arise from incorrect space integration, as it *e.g.* can occur in the atomic sphere approximation. In our implementation of the full-potential, the space is divided into Voronoi polyhedra,<sup>30</sup> which exactly fill up the space without any overlap, so that the space integration is performed exactly. Rather the small deviations arise from an inherent feature of the KKR-Green's function method, which due to the  $\ell_{max}$ -cutoff violates the state normalization. A proper state counting leading to integer numbers for the total charges could only be achieved if all angular momenta up to  $\ell_{max} = \infty$  would be included in the calculation, which is practically impossible in realistic cases. The problem can be overcome by the application of the Lloyd's formula,<sup>35</sup> which contains an implicit summation over all angular momenta, thus yielding the correct total charge and moment. Since the evaluation of Lloyd's

formula is a complex numerical problem, this is usually avoided arising to the above small inconsistencies.

Recently, a member of our group<sup>36</sup> has succeeded in implementing the Lloyd's formula in our Green's function code and we have tested the case of Co<sub>2</sub>MnGe. The calculations give indeed an integer total moment of  $5 \mu_B$  (instead of  $4.941 \mu_B$  in Table I), and the (non-integer) local moments are slightly increased. Most of the charge adjustment occurs in the metallic majority band and the Fermi level is practically unchanged, situated as in Fig. 2 in the minority gap. This is also plausible from energetic point of view; the total energy favors this position of the Fermi level. Based on this experience and on calculations as above with different  $\ell_{max}$  cut-offs, we conclude (i) that in our calculations the correct criterium for half-metallicity is, that the Fermi level is in the minority gap and (ii) that the small deviations of the total moments from integer values are insignificant.

Thus we have verified by the DOS that all compounds under study in this section are half-metals. The compounds containing Al and Ga have 28 valence electrons and the ones containing Si, Ge and Sn 29 valence electrons. The first compounds have a total spin moment of  $4 \mu_B$  and the second ones of  $5 \mu_B$  which agree with the experimental deduced moments of these compounds.<sup>37</sup> So it seems that the total spin moment,  $M_t$ , is given with respect to the total number of valence electrons,  $Z_t$ , from the simple relation:  $M_t = Z_t - 24$ . In the following we will analyze the origin of this rule.

### III. ORIGIN OF THE GAP AND SLATER-PAULING BEHAVIOR

As we mentioned above, the total spin magnetic moments of the Co<sub>2</sub>MnZ compounds follow the  $M_t = Z_t - 24$  rule. A similar relation, *i.e.*  $M_t = Z_t - 18$ , is also found for the half-Heusler compounds.<sup>5,38</sup> Both state nothing more than the well known Slater-Pauling behavior.<sup>39</sup> In such a picture the occupancy of the spin-down bands does not change and the extra or missing electrons are taken care of by the spin-up states only. The 24 means that there are 12 occupied spin-down states, as the total moment, which is the number of uncompensated spins, is given by the total number of valence electrons  $Z_t$  minus two times the number of minority electrons.

In Fig. 3 we present the representations of each one of the bands at the  $\Gamma$  point (see Table II for the different representations). Firstly the *sp* atom creates one *s* band and three *p* bands which are fully occupied. The *s* electrons transform following the  $\Gamma_1$  representation; we do not show this band in Fig. 3 as it is very low in energy and it is well separated by the other bands. The *p* electrons of the *sp* atom transform following the  $\Gamma_{15}$  representation and they hybridize with *p* electrons of the Mn and Co atoms which transform with the same representation. As can be seen in the band structure, these bands are lower than the bands that have mainly *d* character but they

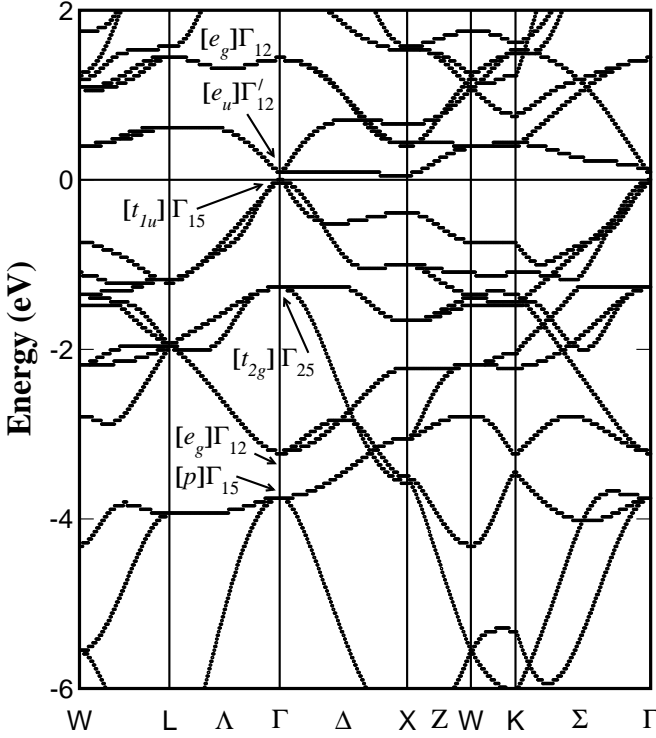


FIG. 3: Spin-down band structure of the  $\text{Co}_2\text{MnGe}$  compound. The indirect gap, present in the half-Heusler alloys, is practically destroyed. For the explanation of the different representations of the group symmetry of the  $\Gamma$  point look at Table II. In brackets we present the type of orbitals transforming following each representation (see Fig. 4).

are not well separated by them (there is a band crossing along the  $\Gamma\text{K}$  direction). As in the half-Heusler alloys,<sup>5</sup> the 4  $sp$  bands can be only partially filled by the  $n$  valence electrons of the  $sp$  atom ( $n = 3$  for Al, Ga or 4 for Si Ge and Sn), so that an additional  $8 - n$   $d$  electrons are accommodated in these bands (4  $d$ -electrons in the case of  $\text{Co}_2\text{MnGe}$  or 5  $d$ -electrons for  $\text{Co}_2\text{MnAl}$ ). Therefore in the Heusler alloys the effective number of  $d$  electrons (in the higher lying  $d$  bands) can be controlled by the valence of the  $sp$  atom. This is a very unusual behavior for metallic systems, which can be used to engineer Heusler alloys with very different magnetic properties (see Section IV).

In the case of the half-Heusler alloys, like  $\text{CoMnSb}$ , there is only one Co atom per unit cell and its  $d$  valence electrons are hybridizing with the Mn ones creating five bonding states below the Fermi level and five antibonding ones above the Fermi level. In the full-Heusler alloys the existence of the second Co atom makes the physics of these systems more complex. As we mentioned above the whole crystal has the tetrahedral symmetry ( $T_d$ ). But if we neglect the Mn and the  $sp$  sites, then the Co atoms themselves sit on a cubic lattice respecting the octahedral symmetry ( $O_h$ ). So there could be states obeying the  $O_h$  being localized exclusively at the Co sites; note here that the  $T_d$  is a subgroup of  $O_h$ . Thus we will take into account firstly the interactions between the two in-

TABLE II: Representations of the real space octahedral ( $O_h$ ) symmetry group (first column). In the second column the corresponding representations of the symmetry group of the  $\Gamma$  point following the nomenclature introduced in Ref. 40. In the third and fourth columns we present the orbitals which transform following each one of the different representations. Notice that the whole crystal has the tetrahedral  $T_d$  symmetry but the lattice consisted only of Co atoms has the  $O_h$  symmetry;  $T_d$  is a subgroup of  $O_h$ . Thus it is possible to have states located only at the Co sites, *e.g.* the  $d$  orbitals transforming according to the  $E_g$  representation. Also the  $d$  hybrids transforming according to the  $T_{1u}$  representation are localized at the Co atoms as there are no  $d$  states at the Mn site with the same representation. The subscripts a and b refer to orbitals at the two different Co sites in the unit cell (look Fig. 1); the 1, 2, 3, 4 and 5 refer to  $d$  orbitals of the  $xy$ ,  $yz$ ,  $zx$ ,  $3z^2 - r^2$  and  $x^2 - y^2$  symmetries, respectively; the 1, 2 and 3 refer to  $p$  orbitals of the  $x$ ,  $y$  and  $z$  symmetries, respectively.

$O_h$	Ref. 40	Co-Co	Mn or Ge
$A_{1g}$	$\Gamma_1$	$s_a + s_b$	$s$
$A_{1u}$	$\Gamma'_1$	$s_a - s_b$	
$E_g$	$\Gamma_{12}$	$d_{ia} + d_{ib}$ [ $i=4,5$ ]	$d_4 d_5$
$E_u$	$\Gamma'_{12}$	$d_{ia} - d_{ib}$ [ $i=4,5$ ]	
$T_{2g}$	$\Gamma_{25}$	$p_{ia} - p_{ib}$ & $d_{ia} + d_{ib}$ [ $i=1,2,3$ ]	$d_1 d_2 d_3$
$T_{1u}$	$\Gamma_{15}$	$p_{ia} + p_{ib}$ & $d_{ia} - d_{ib}$ [ $i=1,2,3$ ]	$p_1 p_2 p_3$

equivalent Co sites and then their interaction with the Mn or the  $sp$  atom, as was also the case for the  $\text{Fe}_2\text{MnZ}$  compounds.<sup>17</sup>

In order to discuss the behavior of the  $d$  electrons in the full Heusler alloys we have drawn schematically in Fig. 4 the possible hybridizations between the different atoms. The  $d_{1...5}$  orbitals correspond to the  $d_{xy}$ ,  $d_{yz}$ ,  $d_{zx}$ ,  $d_{3z^2-r^2}$  and  $d_{x^2-y^2}$  orbitals, respectively. The symbol  $e_g$  means that the orbital transform following the  $E_g$  representation. Note that due to symmetry, the  $e_g$  orbitals at the Co site can only couple with  $e_g$  orbitals at the other Co site or at the Mn site. The same applies for the  $t_{2g}$  orbitals. Looking at Fig. 4 we see firstly that when two neighboring Co atoms interact, their  $d_4$  and  $d_5$  orbitals form bonding  $e_g$  and antibonding  $e_u$  states; the coefficient in front of each orbital is the degeneracy of this orbital. The  $d_1$ ,  $d_2$  and  $d_3$  orbitals of each Co also hybridize creating a triple degenerated bonding  $t_{2g}$  orbital and a triple degenerated antibonding  $t_{1u}$  orbital.

As we show in the second part of Fig. 4, the double degenerated  $e_g$  orbitals hybridize with the  $d_4$  and  $d_5$  of the Mn that transform also with the same representation. They create a double degenerated bonding  $e_g$  state that is very low in energy and an antibonding one that is unoccupied and above the Fermi level. The  $3 \times t_{2g}$  Co orbitals couple to the  $d_{1,2,3}$  of the Mn and create 6 new orbitals, 3 of which are bonding and are occupied and the other three are antibonding and high in energy. Finally the  $2 \times e_u$  and  $3 \times t_{1u}$  Co orbitals cannot couple with any of the Mn  $d$  orbitals as there are none transforming with the  $u$  representations. The  $t_{1u}$  states are below the Fermi

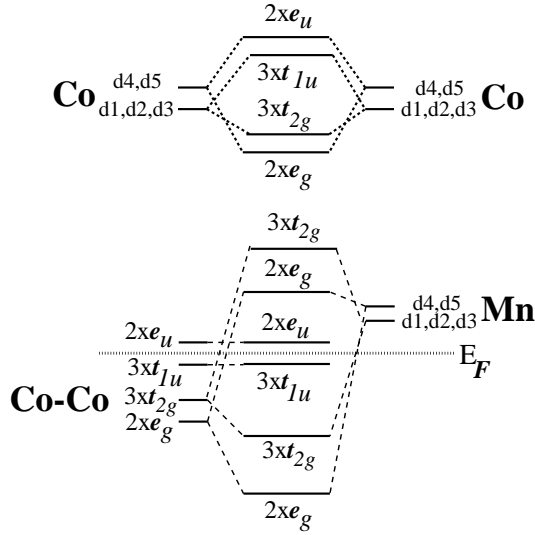


FIG. 4: Possible hybridizations between spin-down orbitals sitting at different sites in the case of the  $\text{Co}_2\text{MnGe}$  compound. To explain the properties of the full Heusler alloys, firstly we consider the hybridization between the two different Co atoms and afterwards the hybridization with the Mn atom. The names of the orbitals follow the nomenclature introduced in Table II. The coefficient represents the degeneracy of each orbital.

level and they are occupied while the  $e_u$  are just above the Fermi level. Thus in total 8 minority  $d$  bands are filled and 7 are empty. Our description is somewhat different from the one in Ref. 17 where it has been assumed that the orbitals just below the Fermi level are also  $t_{2g}$  and not  $t_{1u}$  as in our case. To elucidate this difference we have drawn in Fig. 5 the atomic-resolved  $d$  DOS projected on the double degenerated and the triple degenerated representations. Although we cannot distinguish in our projection the  $t_{2g}$  from the  $t_{1u}$  and the  $e_g$  from the  $e_u$ , around the Fermi level the Mn atom presents a broad spin-down gap which is not present at the Co sites. So minority states around the gap are localized at the Co and do not couple to Mn, and the only states that have this property are the  $t_{1u}$  and the  $e_u$ . Thus the peak below the Fermi level is the  $3 \times t_{1u}$  state and the peak just above the Fermi level is the  $2 \times e_u$  state. This also explains why the gap is small. The two cobalt atoms are second neighbors and their hybridization is not so strong and the splitting of the states is small and thus the energy distance between the  $t_{1u}$  levels and the  $e_u$  ones is small. As these states do not hybridize with the Mn states their splitting does not change and the gap is considerably smaller than the one in the half-Heusler alloys. In the latter compounds we have only one Co atom per unit cell coupling to the Mn atom and so the  $t_{1u}$  and the  $e_u$  states are absent and only the  $e_g$  and  $t_{2g}$  survive. Therefore a real gap exists in the half-Heusler alloys and the minority valence and the minority valence bands contain 9 electrons:  $1 \times s$ ,  $3 \times p$  and  $5 \times d$ .

To summarize, in the case of the full-Heusler alloys we

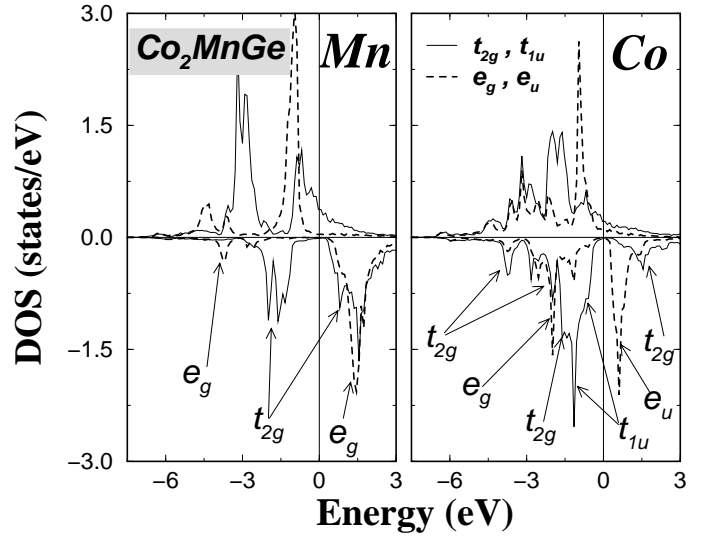


FIG. 5: Projected  $d$  DOS on the double and on the triple degenerated representations for each atom in the  $\text{Co}_2\text{MnGe}$  compound. We also give the character of each peak for the spin-down states. Notice that in the minority bands around the Fermi level there are only Co states.

have 8 occupied minority  $d$  states per unit cell: the double degenerated  $e_g$  very low in energy, the triple degenerated  $t_{2g}$  orbital and finally the triple degenerated  $t_{1u}$  just below the Fermi level. Thus in total we have 12 minority occupied states per unit cell, one with  $s$  character, three with  $p$  character and 8 with  $d$  character. Therefore the total moment obeys the simple rule  $M_t = Z_t - 24$  as compared to  $M_t = Z_t - 18$  for the half-Heusler alloys. Note here that as shown in Fig. 4 we have in total 15 spin-down  $d$  states, meaning 30 in total if we take into account both spin directions, so the states count is correct as each of the two Co atoms and the Mn one contributes totally 10  $d$  states. We can trace these states also in the spin-down band structure analyzing the character of each band at the  $\Gamma$  point. In Table II we have included the representations of the symmetry group of the  $\Gamma$  point in the reciprocal lattice using the nomenclature introduced in Ref. 40. The symmetry point group of the  $\Gamma$  has the same symmetry operations with the  $O_h$ . Firstly as said above we have a  $s$  like band not shown in the figure with a  $\Gamma_1$  state at the  $\Gamma$  point and then we find at  $\Gamma$  a triple degenerated point that has the  $\Gamma_{15}$  representation corresponding to the  $p$  like orbitals. Above this point there is a double-degenerated  $\Gamma_{12}$  point which corresponds to the  $e_g$  orbitals while the other  $e_g$  orbitals for  $\text{Co}_2\text{MnGe}$  are found above the Fermi level and also above the unoccupied  $e_u$  orbitals that correspond to the double degenerated point with the  $\Gamma'_{12}$  symmetry. Finally, there are two triple degenerated points  $\Gamma_{25}$  and  $\Gamma_{15}$  which correspond to the occupied  $t_{2g}$  and  $t_{1u}$  orbitals, respectively, while the other unoccupied  $t_{2g}$  orbitals ( $\Gamma_{25}$ ) are high in energy and are not shown in the figure.

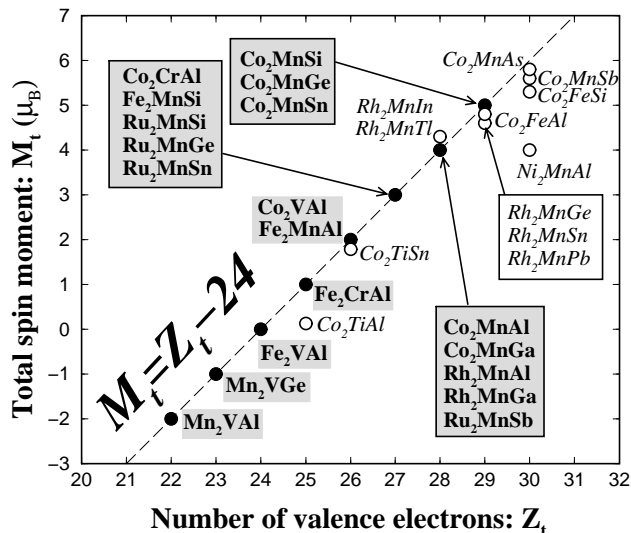


FIG. 6: Calculated total spin moments for all the studied Heusler alloys. The dashed line represents the Slater-Pauling behavior. With open circles we present the compounds deviating from the SP curve. To decide whether one alloy is half-ferromagnet or not, we have used the DOS and not the total spin-moments (see Section II).

From the above discussion we find that in the minority band 7  $d$  states above  $E_F$  are unoccupied. Thus the largest possible moment, which a full-Heusler alloys can have, is  $7 \mu_B$ , since in this case all majority  $d$  states are filled. This is different from the half-Heusler compounds which have five empty  $d$ -states in the minority band and therefore a maximum moment of  $5 \mu_B$ .

#### IV. OTHER FULL-HEUSLER COMPOUNDS FOLLOWING THE SP CURVE

Following the discussion of the previous section we will go on investigating other full-Heusler alloys that can follow the Slater-Pauling curve and in Fig. 6 we have plotted the total spin magnetic moments for all the compounds under study as a function of the total number of valence electrons. The dashed line represents the rule:  $M_t = Z_t - 24$ . In the following we will analyze all these results. Overall we see that many of our results coincide with the Slater-Pauling curve. Some of the Rh compounds show small deviations which are more serious for the  $\text{Co}_2\text{TiAl}$  compound. We see that there is no compound with a total spin moment of  $7 \mu_B$  or even  $6 \mu_B$ . Moreover we found also examples of half-metallic materials with less than 24 electrons,  $\text{Mn}_2\text{VGe}$  with 23 valence electrons and  $\text{Mn}_2\text{VAl}$  with 22 valence electrons.

TABLE III: Calculated spin magnetic moments in  $\mu_B$  using the experimental lattice constants (see Ref. 11) for the full-Heusler alloys containing Co, Fe and Mn.

$m^{\text{spin}}(\mu_B)$	Co,Fe,Mn	Y	Al,Si,Ge	Total
$\text{Co}_2\text{TiAl}$	0.072	-0.013	-0.002	0.130
$\text{Co}_2\text{TiSn}$	0.911	-0.039	0.001	1.784
$\text{Co}_2\text{VAl}$	0.863	0.232	-0.033	1.926
$\text{Co}_2\text{CrAl}$	0.755	1.536	-0.091	2.955
$\text{Co}_2\text{MnAl}$	0.768	2.530	-0.096	3.970
$\text{Co}_2\text{FeAl}$	1.129	2.730	-0.099	4.890
$\text{Fe}_2\text{VAl}$		paramagnet		
$\text{Fe}_2\text{CrAl}$	-0.093	1.108	-0.011	0.910
$\text{Fe}_2\text{MnAl}$	-0.275	2.548	-0.019	1.979
$\text{Fe}_2\text{MnSi}$	0.191	2.589	-0.029	2.943
$\text{Mn}_2\text{VAl}$	-1.413	0.786	0.018	-2.021
$\text{Mn}_2\text{VGe}$	-0.750	0.476	0.021	-1.003

##### A. $\text{Co}_2\text{YAl}$ and $\text{Fe}_2\text{YAl}$ compounds

We have calculated the spin moments of the compounds  $\text{Co}_2\text{YAl}$  where  $Y = \text{Ti, V, Cr, Mn}$  and  $\text{Fe}$  and in Table III we have gathered the atomic and the total spin magnetic moments. There are experimental results only for the moment at the Co site for the Ti, V, and Cr compounds using hyperfine field measurements by Pendl *et al.*<sup>41</sup> and by Carbonari *et al.*<sup>42</sup>, which agree very well with our *ab-initio* results. The compounds containing V, Cr and Mn show a similar behavior. As we substitute Cr for Mn, that has one valence electron less than Mn, we depopulate one Mn spin-up state and thus the spin moment of Cr is around  $1 \mu_B$  smaller than the Mn one while the Co moments are practically the same for both compounds. This behavior is clearly seen in Fig. 7 where we present the atom- and spin-resolved DOS for the two compounds. The minority DOS is the same for both compounds as they follow the SP curve and this is also the case for the Co spin-up DOS. In the case of the Cr compound the Fermi level falls within a broad and large Cr spin-up peak. When we substitute Mn for Cr this peak moves lower in energy to account for the extra electron and the Fermi level is now at the right edge of the peak, but nothing else changes in the calculated DOS. Substituting V for Cr has a larger effect since also the Co spin-up DOS changes slightly and the Co magnetic moment is increased by about  $0.1 \mu_B$  compared to the other two compounds and V possesses a small moment of  $0.2 \mu_B$ . This change in the behavior is due to the smaller hybridization between the Co atoms and the V compared to the Cr and Mn atoms. Although all three  $\text{Co}_2\text{VAl}$ ,  $\text{Co}_2\text{CrAl}$  and  $\text{Co}_2\text{MnAl}$  compounds are on the SP curve as can be seen in Fig. 6, this is not the case for the compounds containing Fe and Ti. If the substitution of Fe for Mn followed the same logic as the one of Cr for Mn then the Fe moment should be around  $3.5 \mu_B$  which is a very large moment for the Fe site. Therefore it is energetically more favorable for the system that also the Co moment is increased, as it was also the case for the

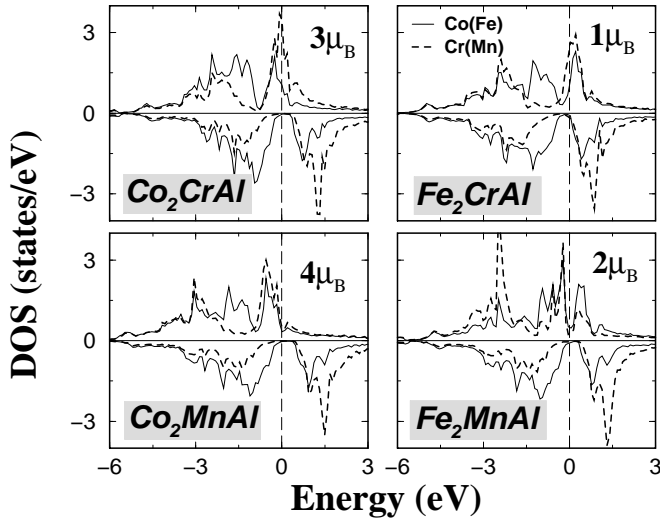


FIG. 7: Calculated atom- and spin-projected DOS for the  $\text{Co(Fe)}_2\text{Mn(Cr)Al}$  compounds. They all present a spin-down pseudogap. The numbers give the total moments.

other systems with 29 electrons like  $\text{Co}_2\text{MnSi}$ , but while the latter one makes it to  $5 \mu_B$ ,  $\text{Co}_2\text{FeAl}$  reaches a value of  $4.9 \mu_B$ . A similar behavior was seen also in the case of the isoelectronic  $\text{Co}_2\text{FeGa}$  compound, but the total spin moment was slightly larger than  $5 \mu_B$ .<sup>33</sup> In the case of  $\text{Co}_2\text{TiAl}$ , it is energetically more favorable to have a weak ferromagnet than an integer moment of  $1 \mu_B$  as it is very difficult to magnetize the Ti atom. Even in the case of the  $\text{Co}_2\text{TiSn}$  the calculated total spin magnetic moment of  $1.78 \mu_B$  (compared to the experimental value of  $1.96 \mu_B$ )<sup>43</sup> arises only from the Co atoms as was also shown experimentally by Pendl *et al.*,<sup>41</sup> and the Ti atom is practically paramagnetic and the latter compound fails to follow the SP curve.

As a second family of materials we have calculated also the compounds containing Fe and we present their total spin moments also in Table III.  $\text{Fe}_2\text{VAl}$  has in total 24 valence electrons and is a semimetal, *i.e.* paramagnetic with a very small DOS at the Fermi level, as it is already known experimentally.<sup>44</sup> All the studied Fe compounds follow the SP behavior as can be seen in Fig. 6. In the case of the  $\text{Fe}_2\text{CrAl}$  and  $\text{Fe}_2\text{MnAl}$  compounds the Cr and Mn atoms have spin moments comparable to the Co compounds and similar DOS as can be seen in Fig. 7. In order to follow the SP curve the Fe in  $\text{Fe}_2\text{CrAl}$  is practically paramagnetic while in  $\text{Fe}_2\text{MnAl}$  it has a small negative moment. When we substitute Si for Al in  $\text{Fe}_2\text{MnAl}$ , the extra electron exclusively populates Fe spin-up states and the spin moment of each Fe atom is increased by  $0.5 \mu_B$  contrary to the corresponding Co compounds where also the Mn spin moment was considerably increased.

Finally we calculated as a test  $\text{Mn}_2\text{VAl}$  and  $\text{Mn}_2\text{VGe}$  which have 22 and 23 valence electrons, respectively, to see if we can reproduce the SP behavior not only for compounds with more than 24, but also for compounds

TABLE IV: Calculated atom-resolved and total spin magnetic moments in  $\mu_B$  using the experimental lattice constants for the full-Heusler alloys containing Rh and Ru (see Ref. 11 for the lattice constants of the Rh compounds and Ref. 26 for the Ru compounds).

$m^{\text{spin}}(\mu_B)$	Ru, Rh	Mn	Z	Total
$\text{Ru}_2\text{MnSi}$	0.028	2.868	0.025	2.948
$\text{Ru}_2\text{MnGe}$	0.002	2.952	0.021	2.977
$\text{Ru}_2\text{MnSn}$	-0.051	3.137	-0.001	3.034
$\text{Ru}_2\text{MnSb}$	0.222	3.495	0.018	3.957
$\text{Rh}_2\text{MnAl}$	0.328	3.388	-0.041	4.004
$\text{Rh}_2\text{MnGa}$	0.312	3.461	-0.033	4.052
$\text{Rh}_2\text{MnIn}$	0.269	3.720	-0.034	4.223
$\text{Rh}_2\text{MnTl}$	0.266	3.765	-0.027	4.270
$\text{Rh}_2\text{MnGe}$	0.421	3.672	0.011	4.525
$\text{Rh}_2\text{MnSn}$	0.393	3.831	-0.010	4.607
$\text{Rh}_2\text{MnPb}$	0.383	3.888	-0.009	4.644

with less than 24 electrons. As we have already shown  $\text{Fe}_2\text{VAl}$  is paramagnetic and  $\text{Co}_2\text{VAl}$ , which has two electrons more, has a spin moment of  $2 \mu_B$ .  $\text{Mn}_2\text{VAl}$  has two valence electrons less than  $\text{Fe}_2\text{VAl}$  and as we show in Table III its total spin moment is  $-2 \mu_B$ , in agreement with previous ab-initio results,<sup>34</sup> and thus it follows the SP behavior. To our knowledge there is no compound with 23 valence electrons, which has been studied experimentally, so we decided to calculate  $\text{Mn}_2\text{VGe}$  using the lattice constant of  $\text{Mn}_2\text{VAl}$ . We have chosen this compound, because as can be seen in Ref. 11 the compounds containing Al and Ge have practically the same lattice constants. We found that adding one electron to  $\text{Mn}_2\text{VAl}$  results in a decrease of the absolute value of both the Mn and V spin moments (note that V and Mn are antiferromagnetically coupled) so that the resulting  $\text{Mn}_2\text{VGe}$  total spin magnetic moment is  $-1 \mu_B$  following the SP curve as can be also seen in Fig. 6.

## B. The Ru and Rh compounds

To investigate further the Slater-Pauling behavior of the full-Heusler alloys we studied the ones containing a  $4d$  transition metal atom. As we have already mentioned in Section I the Ru compounds are antiferromagnets with Néel temperatures that reach room temperature. We have calculated their properties assuming that they are ferromagnets and present the calculated spin-magnetic moments in Table IV. The  $\text{Ru}_2\text{MnSi}$ ,  $\text{Ru}_2\text{MnGe}$  and  $\text{Ru}_2\text{MnSn}$  have a total spin magnetic moment of  $3 \mu_B$  and  $\text{Ru}_2\text{MnSb}$  a moment of  $4 \mu_B$  following the rule for the magnetic moments that we have already shown for the Co and Fe compounds and thus the Fermi level falls within the pseudogap contrary to the calculations in Ref. 45 where the Fermi level was above the gap. In the case of the alloys with Si, Ge and Sn the Ru atom has a practically zero spin moment and the total moment is carried by the Mn atoms. In Fig. 8 we have drawn the atomic and

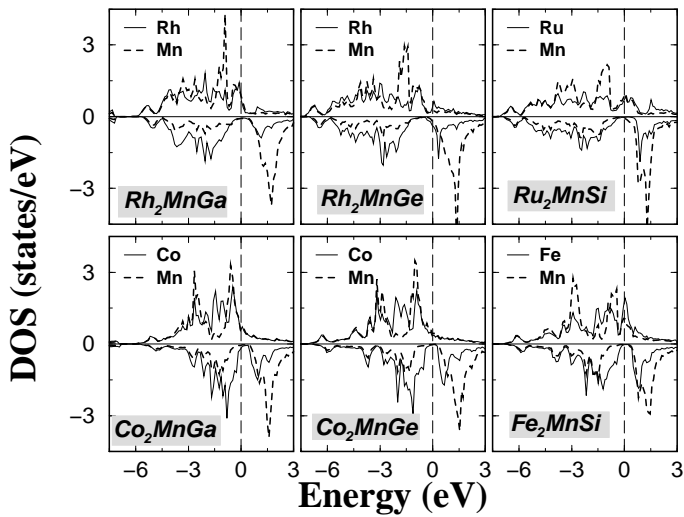


FIG. 8: Calculated atom- and spin-projected DOS for some of the Heusler alloys containing Ru and Rh compared to the alloys containing Fe or Co that are isoelectronic to Ru and Rh, respectively. In the case of the Rh or Ru compounds, the hybridization with the spin-down Mn states is smaller resulting in larger Mn spin moments (see Table IV).

spin DOS for the  $\text{Ru}_2\text{MnSi}$  compound compared to the isoelectronic  $\text{Fe}_2\text{MnSi}$  compound. We see clearly from the DOS that the hybridization between the Mn and Ru spin-down states is smaller than in the case of the Fe compound resulting in a larger Mn spin moment. Although Ru has a practically zero spin moment, we see that the Fermi level falls within a broad peak of spin-up DOS. In the case of  $\text{Ru}_2\text{MnSb}$  this peak is completely occupied resulting in an important induced spin moment at the Ru site that couples ferromagnetically to the Mn one.

The next family of compounds that we have studied are the ones containing Rh and Mn.<sup>25,46</sup> In Table IV we present the calculated spin magnetic moments. As can be seen in Fig. 8 the hybridization between the Rh and the Mn spin-down states is smaller than in the case of the isoelectronic Co compounds, *i.e.* there are Mn states in the Co compound that become Rh states in the Rh compound, thus leading to an increase of the Mn moment, and a decrease of the Rh moment compared to the Co spin moment. This phenomenon is quite intense as the Mn moment increases in all cases more than  $0.6 \mu_B$ . From the studied compounds only  $\text{Rh}_2\text{MnAl}$  and  $\text{Rh}_2\text{MnGa}$  are exactly on the SP curve presented in Fig. 6. The  $\text{Rh}_2\text{MnIn}$  and  $\text{Rh}_2\text{MnTl}$  that are isoelectronic to the two previous compounds have a total spin moment of around  $4.2 - 4.3 \mu_B$ , thus the Fermi level is slightly below the pseudogap in these compounds. In the case of  $\text{Rh}_2\text{MnGe}$ ,  $\text{Rh}_2\text{MnSn}$  and  $\text{Rh}_2\text{MnPb}$ , that possess 29 valence electrons, the total spin moment is around  $4.6 \mu_B$  slightly smaller than the ideal  $5 \mu_B$  and the Fermi level is slightly above the pseudogap. This is proba-

TABLE V: Calculated spin moments for full-Heusler alloys containing 30 valence electrons per unit cell. The experimental lattice parameters were taken from Ref. 11.

$m^{\text{spin}}(\mu_B)$	X	Y	Z	Total
$\text{Ni}_2\text{MnAl}$	0.364	3.359	-0.062	3.973
$\text{Co}_2\text{FeSi}$	1.271	2.756	-0.031	5.268
$\text{Co}_2\text{MnSb}$	1.113	3.401	-0.007	5.620
$\text{Co}_2\text{MnAs}$	1.219	3.309	0.035	5.782

bly due to the considerably larger lattice constant of the Rh compounds with respect to the isoelectronic Co ones. But in general, as can be seen also in Fig. 6, where we summarize all our results, all the compounds are not very far from the SP curve and the deviations are small.

### C. Compounds with 30 valence electrons

As stated in Section III the maximal moment of a full-Heusler alloy is  $7 \mu_B$ , and should occur, when all 15 majority  $d$  states are occupied. Analogously for a half-Heusler alloy the maximal moment is  $5 \mu_B$ . However this limit is difficult to achieve, since due to the hybridization of the  $d$  states with empty  $sp$ -states of the transition metal atoms (sites X and Y in Fig. 1),  $d$ -intensity is transferred into states high above  $E_F$ , which are very difficult to occupy. While we could identify in a recent paper on half-Heusler alloys (Ref. 5) systems with a moment of nearly  $5 \mu_B$ , the hybridization is much stronger in the full-Heusler alloys so that a total moment of  $7 \mu_B$  seems to be impossible. Therefore we restrict our search to possible systems with  $6 \mu_B$ , *i.e.* systems with 30 valence electrons. We have studied some of the possible candidates and we present our results in Table V. One obvious way to reach the 30 electrons is to substitute, *e.g.* in  $\text{Co}_2\text{MnAl}$ , Co by Ni, but Ni is practically paramagnetic and cannot carry a large spin moment and thus the total spin magnetic moment of  $\text{Ni}_2\text{MnAl}$  is only  $4 \mu_B$  far away from the ideal  $6 \mu_B$ . The second way to achieve 30 electrons is to use Fe at the Y site as in the case for the  $\text{Co}_2\text{FeSi}$  compound. Already  $\text{Co}_2\text{FeAl}$  was not reaching the  $5 \mu_B$  and adding one more electron can not increase the total spin moment by more than  $1 \mu_B$ . Although the Co moment reaches the  $1.3 \mu_B$  the Fe moment stays unchanged and the total spin moment is increased only by  $\sim 0.4 \mu_B$  reaching the  $5.3 \mu_B$  instead of the ideal  $6 \mu_B$ .

Our last test cases are the  $\text{Co}_2\text{MnSb}$  and  $\text{Co}_2\text{MnAs}$  compounds. We have calculated  $\text{Co}_2\text{MnSb}$  using the lattice constant of  $\text{Co}_{1.5}\text{MnSb}$  as  $\text{Co}_2\text{MnSb}$  does not really exist. Adding Co to  $\text{Co}_{1.5}\text{MnSb}$  results to the creation of a Co rich phase.  $\text{Co}_2\text{MnSn}$  has a total spin moment of  $5 \mu_B$ . The additional electron increases both the Co and Mn spin moments and the total moment is now  $5.6 \mu_B$ . To our knowledge there is no experimental work on  $\text{Co}_2\text{MnAs}$  and we have calculated it using the lattice constant of  $\text{Co}_2\text{MnGe}$ . This lattice constant should be very



close to the real one as also substituting Ga for Ge only marginally changes it. As shown in Table V the calculated total spin moment is  $5.8 \mu_B$ . But for both compounds if we increase their lattice constant by 4% the Fermi level moves deeper in energy, as was the case also for the half-Heusler alloys,<sup>5</sup> and now it falls within the pseudogap and the total spin moment for both of them reaches the ideal value of  $6 \mu_B$ . So if both  $\text{Co}_2\text{MnSb}$  and  $\text{Co}_2\text{MnAs}$  can be grown on top of a substrate with the appropriate lattice constant using a technique like Molecular Beam Epitaxy, it is possible to get a material with a total spin moment of  $6 \mu_B$  where the Fermi level will be within the pseudogap. In such a case, of course, there is the possibility that the lattice parameter along the growth axis is contracted to account for the large in-plane lattice parameter, which can lead to a change of the total spin moment.

## V. CONCLUSIONS

Using the full-potential screened Korringa-Kohn-Rostoker method we studied the full-Heusler alloys containing Co, Fe, Rh and Ru. We have shown using the scalar-relativistic approximation that for all these com-

pounds the top edge of the highest occupied spin-down band and the bottom edge of the lowest unoccupied spin-down band touch the Fermi level practically destroying the indirect gap. These compounds show a Slater-Pauling behavior and the total spin-magnetic moment per unit cell ( $M_t$ ) scales with the total number of valence electrons ( $Z_t$ ) following the rule:  $M_t = Z_t - 24$ . The Co-Co hybridization is primordial to explain why the spin-down band contains exactly 12 electrons and why only a tiny gap exists in these compounds. Finally we have shown that it is possible to find the Slater-Pauling behavior even for materials with less than 24 valence electrons like  $\text{Mn}_2\text{VAl}$  and  $\text{Mn}_2\text{VGe}$ , and that the compounds with 30 valence electrons are unlikely to achieve a total spin moment of  $6 \mu_B$ .

## Acknowledgments

The authors acknowledge financial support from the RT Network of *Computational Magnetoelectronics* (contract RTN1-1999-00145) of the European Commission. We thank Dr. Rudi Zeller for providing us with a version of the KKR code incorporating the Lloyd's formula and for helpful discussions.

---

\* Electronic address: I.Galanakis@fz-juelich.de

- <sup>1</sup> S. A. Wolf, D. D. Awschalom, R. A. Buhrman, J. M. Daughton, S. von Molnár, M. L. Roukes, A. Y. Chtchelkanova, and D. M. Treger, *Science* **294**, 1488 (2001); G. A. Prinz, *Science* **282**, 1660 (1998); G. A. Prinz, *J. Magn. Magn. Mater.* **200**, 57 (1999).
- <sup>2</sup> R. A. de Groot, F. M. Mueller, P. G. van Engen, and K. H. J. Buschow, *Phys. Rev. Lett.* **50**, 2024 (1983).
- <sup>3</sup> E. Kulatov and I. I. Mazin, *J. Phys.: Condens. Matter* **2**, 343 (1990); S. V. Halilov and E. T. Kulatov, *J. Phys.: Condens. Matter* **3**, 6363 (1991); X. Wang, V. P. Antropov, and B. N. Harmon, *IEEE Trans. Magn.* **30**, 4458 (1994). S. J. Youn and B. I. Min, *Phys. Rev. B* **51**, 10 436 (1995); V. N. Antonov, P. M. Oppeneer, A. N. Yaresko, A. Ya. Perlov, and T. Kraft, *Phys. Rev. B* **56**, 13 012 (1997).
- <sup>4</sup> I. Galanakis, S. Ostanin, M. Alouani, H. Dreyssé, and J. M. Wills, *Phys. Rev. B* **61**, 4093 (2000).
- <sup>5</sup> I. Galanakis, P. H. Dederichs, and N. Papanikolaou, *arXiv:cond-mat/0203534*.
- <sup>6</sup> K. E. H. M. Hanssen and P. E. Mijnders, *Phys. Rev. B* **34**, 5009 (1990); K. E. H. M. Hanssen, P. E. Mijnders, L. P. L. M. Rabou, and K. H. J. Buschow, *Phys. Rev. B* **42**, 1533 (1990).
- <sup>7</sup> M. N. Kirillova, A. A. Makhnev, E. I. Shreder, V. P. Dyakina, and N. B. Gorina, *Phys. Stat. Sol. (b)* **187**, 231 (1995).
- <sup>8</sup> P. Turban, S. Andrieu, B. Kierren, E. Snoeck, C. Teodorescu, and A. Traverse, *Phys. Rev. B* **65**, 134417 (2002); D. Ristoiu, J. P. Nozières, C. N. Borca, T. Komesu, H.-K. Jeong, and P.A. Dowben, *Europhys. Lett.* **49**, 624 (2000); W. van Roy, J. de Boeck, B. Brijs, and G. Borghs, *Appl. Phys. Lett.* **77**, 4190 (2000).
- <sup>9</sup> G. A. Wijs and R. A. de Groot, *Phys. Rev. B* **64**, R020402 (2001); S. J. Jenkins and D. A. King, *Surf. Sci.* **494**, L793 (2001); S. J. Jenkins and D. A. King, *Surf. Sci.* **501**, L185 (2002).
- <sup>10</sup> I. Galanakis, *J. Phys.: Condens. Matter* **14**, 6329 (2002).
- <sup>11</sup> P. J. Webster and K. R. A. Ziebeck, in *Alloys and Compounds of d-Elements with Main Group Elements. Part 2.*, edited by H. R. J. Wijn, Landolt-Boörnstein, New Series, Group III, Vol. 19/c (Springer, Berlin), 1988, pp. 75-184.
- <sup>12</sup> K. R. A. Ziebeck and K.-U. Neumann, in *Magnetic Properties of Metals*, edited by H. R. J. Wijn, Landolt-Boörnstein, New Series, Group III, Vol. 32/c (Springer, Berlin), 2001, pp. 64-414.
- <sup>13</sup> J. Kübler, A. R. Williams, and C. B. Sommers, *Phys. Rev. B* **28**, 1745 (1983).
- <sup>14</sup> P. J. Webster, *J. Phys. Chem. Solids* **32**, 1221 (1971); K. R. A. Ziebeck and P. J. Webster, *J. Phys. Chem. Solids* **35**, 1 (1974).
- <sup>15</sup> S. Ishida, S. Akazawa, Y. Kubo, and J. Ishida, *J. Phys. F: Met. Phys.* **12**, 1111 (1982); S. Ishida, S. Fujii, S. Kashiwagi, and S. Asano, *J. Phys. Soc. Jpn.* **64**, 2152 (1995).
- <sup>16</sup> S. Fujii, S. Sugimura, S. Ishida, and S. Asano, *J. Phys.: Condens. Matter* **2**, 8583 (1990).
- <sup>17</sup> S. Fujii, S. Ishida, and S. Asano, *J. Phys. Soc. Jpn.* **64**, 185 (1995).
- <sup>18</sup> P. J. Brown, K. U. Neumann, P. J. Webster, and K. R. A. Ziebeck, *J. Phys.: Condens. Matter* **12**, 1827 (2000).
- <sup>19</sup> T. Ambrose, J. J. Krebs, and G. A. Prinz, *Appl. Phys. Lett.* **76**, 3280 (2000); T. Ambrose, J. J. Krebs, and G. A. Prinz, *J. Appl. Phys.* **87**, 5463 (2000).
- <sup>20</sup> F. Y. Yang, C. H. Shang, C. L. Chien, T. Ambrose, J. J. Krebs, G. A. Prinz, V. I. Nikitenko, V. S. Gornakov, A. J.

- Shapiro, and R. D. Shull, Phys. Rev. B **65**, 174410 (2002).
- <sup>21</sup> M. P. Raphael, B. Ravel, M. A. Willard, S. F. Cheng, B. N. Das, R. M. Stroud, K. M. Bussmann, J. H. Claassen, and V. G. Harris, Appl. Phys. Lett. **79**, 4396 (2001).
  - <sup>22</sup> B. Ravel, M. P. Raphael, V. G. Harris, and Q. Huang, Phys. Rev. B **65**, 184431 (2002).
  - <sup>23</sup> U. Geiersbach, A. Bergmann, and K. Westerholt, J. Magn. Magn. Mater. **240**, 546 (2002).
  - <sup>24</sup> S. Ishida, T. Masaki, S. Fujii, and S. Asano, Physica B **245**, 1 (1998).
  - <sup>25</sup> J. C. Suits, Phys. Rev. B **14**, 4131 (1976).
  - <sup>26</sup> T. Kanomata, M. Kikuchi, H. Yamauchi, and T. Kaneko, Jpn. J. Appl. Phys. **32** Suppl **32-33**, 292 (1993).
  - <sup>27</sup> M. Gotoh, M. Phashi, T. Kanomata, and Y. Yamaguchi, Physica B **213&214**, 306 (1995).
  - <sup>28</sup> S. Ishida, S. Kashiwagi, S. Fujii, and S. Asano, Physica B **210**, 140 (1995).
  - <sup>29</sup> I. Galanakis, Phys. Rev. B Phys. Rev. B **66**, 012406 (2002).
  - <sup>30</sup> N. Papanikolaou, R. Zeller, and P. H. Dederichs, J. Phys.: Condens. Matter **14**, 2799 (2002).
  - <sup>31</sup> S. H. Vosko, L. Wilk, and N. Nusair, Can. J. Phys. **58**, 1200 (1980).
  - <sup>32</sup> D. Brown, M. D. Crapper, K. H. Bedwell, M. T. Butterfield, S. J. Guilfoyle, A. E. R. Malins, and M. Petty, Phys. Rev. B **57**, 1563 (1998).
  - <sup>33</sup> A. Deb, M. Itou, Y. Sakurai, N. Hiraoka, and N. Sakai, Phys. Rev. B **63**, 064409 (2001).
  - <sup>34</sup> R. Weht and W. E. Pickett, Phys. Rev. B **60**, 13006 (1999).
  - <sup>35</sup> P. Lloyd, Proc. Phys. Soc. London **90**, 207 (1967); *idem* **90**, 217 (1967); G. Lehman, Phys. Status Solidi B **70**, 737 (1975); B. Drittler, M. Weinert, R. Zeller, and P. H. Dederichs, Phys. Rev. B **39**, 930 (1989); A. F. Tatarchenko and N. I. Kulikov, Phys. Rev. B **50**, 8266 (1994).
  - <sup>36</sup> R. Zeller, private communication.
  - <sup>37</sup> R. A. Dunlap and D. F. Jones, Phys. Rev. B **26**, 6013 (1982); S. Plogmann, T. Schlathölter, J. Braun, M. Neumann, Yu. M. Yarmoshenko, M. V. Yablonskikh, E. I. Shreder, E. Z. Kurmaev, A. Wrona, and A. Ślebarski, Phys. Rev. B **60**, 6428 (1999).
  - <sup>38</sup> D. Jung, H.-J. Koo, and M.-H. Whangbo, J. Mol. Struct. (Theochem) **527**, 113 (2000).
  - <sup>39</sup> J. Kübler, Physica B **127**, 257 (1984).
  - <sup>40</sup> L. P. Bouckaert, R. Smoluchowski, and E. Wigner, Phys. Rev. **50**, 58 (1936).
  - <sup>41</sup> W. Pendl Jr., R. N. Saxena, A. W. Carbonari, J. Mestnik Filho, and J. Schaff, J. Phys.: Condens. Matter **8**, 11317 (1996).
  - <sup>42</sup> A. W. Carbonari, R. N. Saxena, W. Pendl, Jr. J. Mestnik Filho, R. N. Attili, M. Olzon-Dionysio, and S. D. de Souza, J. Magn. Magn. Mater. **163**, 313 (1996).
  - <sup>43</sup> P. G. van Engen, K. H. J. Buschow, and M. Erman, J. Magn. Magn. Mater. **30**, 374 (1983).
  - <sup>44</sup> Ye Feng, J. Y. Rhee, T. A. Wiener, D. W. Lynch, B. E. Hubbard, A. J. Sievers, D. L. Schlagel, T. A. Lograsson, and L. L. Miller, Phys. Rev. B **63**, 165109 (2001); C. S. Lue, J. H. Ross Jr., K. D. D. Rathnayaka, D. G. Naulge, S. Y. Wu and W.-H. Li, J. Phys.: Condens. Matter **13**, 1585 (2001); Y. Nishino, H. Kato, M. Kato, U. Mizutani, Phys. Rev. B **63**, 233303 (2001); A. Matsushita, T. Naka, Y. Takanao, T. Takeuchi, T. Shishido, and Y. Yamada, Phys. Rev. B **65**, 075204 (2002).
  - <sup>45</sup> M. Pugacheva and A. Jezierski, J. Magn. Magn. Mater. **151**, 202 (1995).
  - <sup>46</sup> S. Jha, H. M. Seyoun, G. M. Julian, R. A. Dunlap, A. Vasquez, J. G. M. da Cunha, and S. M. M. Ramos, Phys. Rev. B **32**, 3279 (1985).